

---

# A Cell-Culture Reactor for the On-Line Evaluation of Radiopharmaceuticals: Evaluation of the Lumped Constant of FDG in Human Glioma Cells

Thomas Noll, Heinz Mühlensiepen, Ralf Engels, Kurt Hamacher, Manfred Papaspyrou, Karl-Josef Langen, and Manfred Biselli

*Institutes of Biotechnology, Medicine, and Nuclear Chemistry and Department of Electronics, Jülich Research Center, Jülich, Germany*

---

A fluidized-bed cell-culture reactor with on-line radioactivity detection was developed for the *in vitro* evaluation of radiopharmaceuticals. The technique was applied to measure the dependency of the lumped constant (LC) of FDG on the glucose concentration in the culture medium in a human glioma cell line. **Methods:** Human glioblastoma cells (86HG39) immobilized in open porous microcarriers were cultivated in a continuously operating fluidized-bed bioreactor. At different glucose concentrations in the culture medium, step inputs (0.1 MBq/mL) of FDG were performed and the cellular uptake of FDG was measured on-line and compared with analyzed samples. From these results, the LC of FDG and its dependency on the glucose concentration were calculated. **Results:** This fluidized-bed technique enabled precise and reproducible adjustment of all relevant experimental parameters, including radiotracer time-concentration course, medium composition, pH, dissolved oxygen and temperature under steady-state conditions, and an on-line determination of the intracellular radiotracer uptake. The immobilized glioma cells formed stable, 3-dimensional, tumor-like spheroids and were continuously proliferating, as proven by an S-phase portion of 25%–40%. For further examination of the cells, an enzymatic method for detachment from the carriers without cellular destruction was introduced. In the FDG experiments, a significant dependency of the LC on the glucose level was found. For normoglycemic glucose concentrations, the LC was determined to be in the range of  $0.7 \pm 0.1$ , whereas in hypoglycemia LC increased progressively up to a value of  $1.22 \pm 0.01$  at a glucose concentration of 3 mmol/L. **Conclusion:** The bioreactor represents an improved *in vitro* model for the on-line evaluation of radiotracers and combines a wide range of experimental setups and 3-dimensional, tissue-like cell cultivation with a technique for on-line radioactivity detection.

**Key Words:** cell culture; FDG; fluidized bed; *in vitro*; lumped constant

**J Nucl Med 2000; 41:556–564**

---

**D**espite much discussion, substantial effort, and growing ethical issues, animal models remain the standard for pharmacologic and toxicologic testing. This is mainly be-

cause of the difficulties inherent in attempting to use *in vitro* methods to reproduce the complexity of interactions in living animals (1). But there are also distinct disadvantages to animal models. They provide little information about the controlling mechanisms underlying the mode of action of drugs and, even more important, cannot guarantee reliable extrapolation of effects to humans (2).

*In vitro* methods have some evident advantages over animal models (3,4). There are no ethical objections and, because of the exactly defined and reproducible experimental conditions, a mechanistic interpretation of the results is often possible. Human cells can be used, which allows transfer of the results to humans. In some cases, continuous real-time measurements can be performed. Finally, *in vitro* methods are generally less expensive than *in vivo* methods.

On the other hand, there are disadvantages to *in vitro* models. Most such systems are static and do not permit an appropriate simulation of the time course of drug concentrations in the body. Another problem of most *in vitro* systems is that cells are often cultivated in an unphysiologic manner (e.g., in a 2-dimensional monolayer instead of in 3-dimensional tissues in the organism). This leads in many cases to alterations in cellular reactions and metabolism. One approach that offers the advantages of the *in vitro* method and overcomes some of the disadvantages is cell growth in a 3-dimensional matrix, which can result in more natural metabolic and growth behavior and provide a potential basis for mimicking important aspects of organ structure (5). This has been described for human gliomas, which show distinct differences in their extracellular matrix when grown as tumor spheroids and as monolayers (6). The extracellular matrix plays an important role in cell proliferation and cell differentiation (7,8) and has been suggested to influence penetration barriers to various cytostatic drugs (9,10).

The fluidized-bed cell-culture reactor is a well-established tool for the production of monoclonal antibodies or therapeutic proteins using animal cells (11,12). This technique of 3-dimensional cell cultivation in open porous microcarriers offers several features that may overcome major drawbacks of other *in vitro* systems: precise, flexible, and adjustable experimental conditions; physiologic *in vivo*-like cell culti-

---

Received Jan. 4, 1999; revision accepted Jul. 21, 1999.  
For correspondence or reprints contact: Manfred Biselli, PhD, Institute of Biotechnology, Forschungszentrum Jülich GmbH, Jülich D-52425, Germany.

vation; feasibility of cell and medium sampling; on-line measurement, representative of in vivo-like exposure of the cells to the drug; and continuous operation under steady-state conditions. In this study we extended this system to the on-line evaluation of radiopharmaceuticals.

The high cell densities in the bioreactor allow an easy and accurate determination of changes in the concentration of unlabeled substrates, a process that is difficult in most in vitro systems using low cell densities in monolayer cultivation, such as microtiter plates, tissue flasks, or Leighton tubes. This high sensitivity of the bioreactor method allows determination of metabolic rates similar to those in isolated organs or living animals.

FDG PET is being used in determination of the regional metabolic rate of glucose in the human body and has been found to be useful in many clinical applications, such as the diagnosis and grading of malignant gliomas (13–16). FDG and glucose are transported between blood and brain tissues by the same carrier. In the cytoplasm they compete for hexokinase, which phosphorylates to their respective hexose-6-phosphates. Whereas glucose-6-phosphate is further metabolized, FDG-6-phosphate is trapped in the cell, because the phosphatase activity in the brain is negligible.

Because FDG and glucose differ in their rates of transport and phosphorylation, estimation of the metabolic rate of glucose ( $MR_{Glc}$ ) from the net flux of FDG ( $MR_{FDG}$ ) requires a proportionality constant, the lumped constant (LC), expressed as:

$$LC = \frac{MR_{FDG}}{MR_{Glc}} \quad \text{Eq. 1}$$

An erroneous underestimation of LC will automatically yield a correspondingly erroneous overestimation for  $MR_{Glc}$  (17). The LC in normal whole human brain has been estimated to be in the range of 0.5 (18,19) or 0.86 (17), whereas for gliomas significantly higher values, from 0.7 to 3.1, were found (17). The LC also depends on the plasma glucose concentration because of the different affinities of hexokinase for transport and phosphorylation (20–23).

To test the potential of the fluidized-bed cell-culture reactor for the evaluation of radiopharmaceuticals we studied the kinetics of FDG in human glioma cells and analyzed the influence of the glucose level on the LC of FDG.

## MATERIALS AND METHODS

### Organism and Cultivation Conditions

The glioblastoma cell line 86HG39, which was described by means of immunocytochemical and morphologic criteria (24), was obtained from Dr. Thomas Bilzer (Institut für Neuropathologie Heinrich-Heine-Universität, Düsseldorf, Germany). Cells were grown in Iscove's modified Dulbecco's medium supplemented with 10% fetal calf serum, 100 IU/mL penicillin, and 100 µg/mL streptomycin (all from Gibco/BRL, Eggenstein, Germany) and divided twice a week in ratios between 1:4 and 1:10, depending on

the proliferation rate. Batch cultivations were performed in a humidified atmosphere (37°C; 5% CO<sub>2</sub>).

### Fluidized-Bed Reactor

The fluidized-bed cell-culture reactor consisted of a reactor tube with a thermostat and a conical bottom inlet. The tube was inserted in a recycle loop containing the recirculation pump, dissolved oxygen (DO) probe, external oxygenator for bubble-free aeration through gas-permeable silicone tubing, an application port for injecting the radiotracer, and a sampling port for medium and carriers (Fig. 1). Fresh medium was added continuously at rates in accordance with cell consumption, which was measured periodically from medium samples, and supernatant was simultaneously removed. Temperature and pH were adjusted to 37°C and 7.2, respectively, and the DO concentration was controlled at 30% of air saturation by adding oxygen or nitrogen using mass flow valves.

The cells were immobilized on open, porous borosilicate glass carriers (Siran; Schott, Mainz, Germany) modified with gelatin (25), with a diameter of 400–500 µm and a porosity of 50%. The reactor had a total volume of 98 mL, and the volume of settled carriers was 30 mL. The bioreactor tube was equipped with 2 detectors, consisting of a NaI scintillator, a photomultiplier, and an amplifier. They were connected to a standard readout electronic display (main amplifier, discriminator, and counter), allowing simultaneous data recording in time steps as short as 1 s. One detector faced the fluidized bed and the other faced the medium (Fig. 1). This arrangement enabled on-line determination of the intracellular tracer accumulation. The difference between the 2 detectors, taking into account the attenuating effect of the glass portion of the fluidized bed, was equivalent to the tracer uptake of the cells.

Dosage of the radiopharmaceuticals can be varied in a wide range with this setup. A step function could be performed as well as a pulse input or an exactly defined profile using a perfusor. To perform a step input, 200 mL supernatant were collected during the steady state of the fermentation, centrifuged (10 min at 2000g), and filtered. Radiotracer was added to the filtrate in an amount to give the intended concentration (0.1 MBq/mL), and the solution was used to replace the medium in the reactor within 25 s.

Samples of medium or carriers with immobilized cells were removed through the sampling port; alternatively, samples could be taken through the top in a laminar flow hood. The volumetric flow rate of the circulating medium could be adjusted from 10 to 116 mL/min, corresponding to a medium velocity of 5–57.7 cm/min in the reactor tube, depending on the target of the experiment.

### Analysis

To determine the concentration and viability of cells in tissue flasks, the medium was withdrawn, and the cells were washed once with phosphate-buffered saline (PBS) without calcium and magnesium, pH 7.2 (Gibco/BRL), and detached by trypsinization (5 min at 37°C with a solution of 0.5 g/L trypsin and 0.2 g/L ethylenediaminetetraacetic acid). The cell number was determined in a hemocytometer using the erythrosin B exclusion method (26).

For determination of the number of immobilized cells in the fluidized bed, a volume of approximately 0.5 mL open porous microcarriers was taken from the reactor. The medium was quickly withdrawn and the carriers were washed once with 2 mL PBS. After addition of 5 mL solution of 0.1 mol/L citric acid, 0.1% (wt/vol) crystal violet, and 1% (wt/vol) t-octylphenoxypolyethoxy-

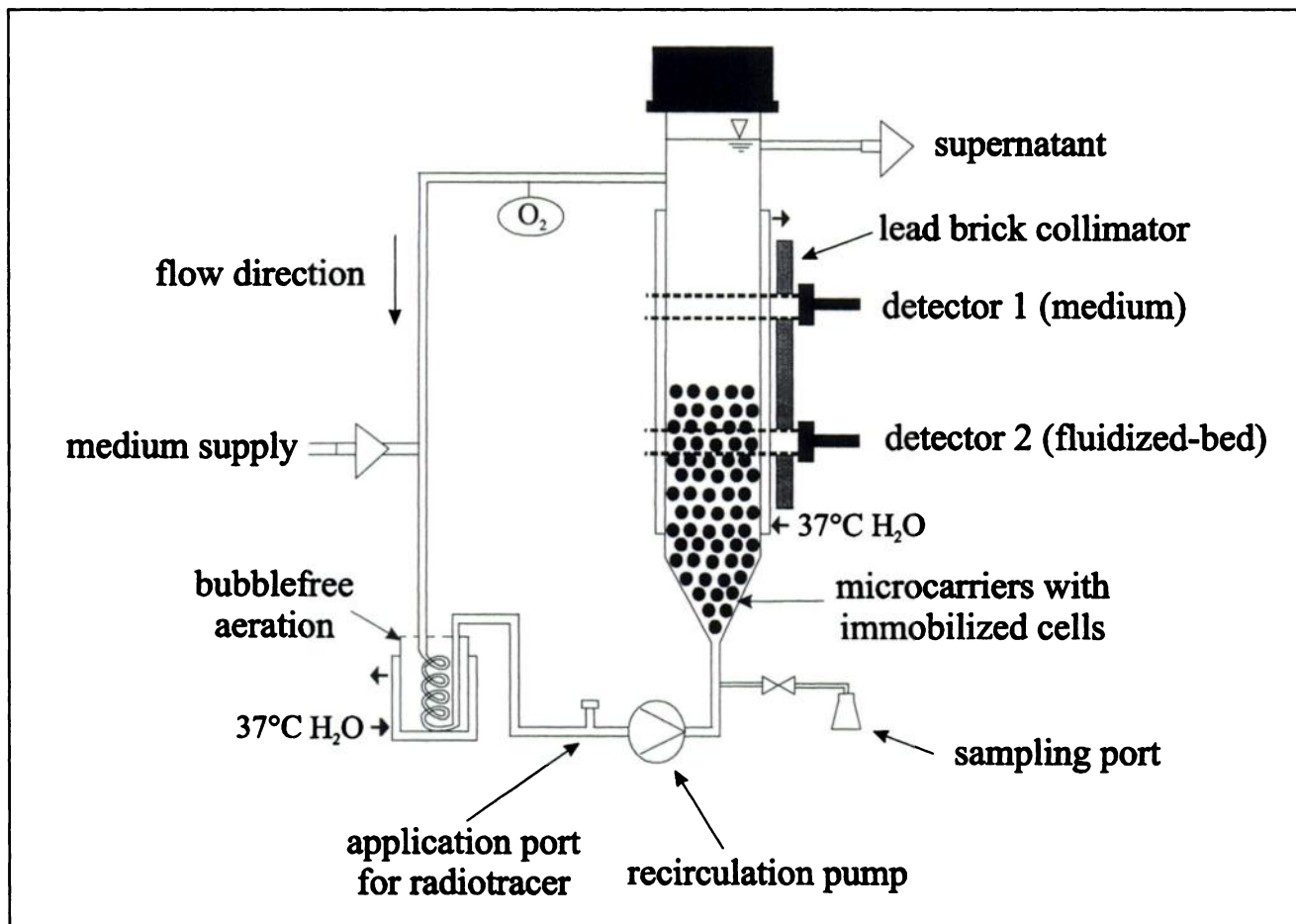


FIGURE 1. Flow sheet of fluidized-bed bioreactor, equipped with 2  $\gamma$  scintillation detectors.

ethanol (Triton X-100; Boehringer Ingelheim, Heidelberg, Germany), the sample was shaken vigorously and incubated at 37°C. After a 6-h incubation, the violet-colored nuclei were counted in a hemocytometer. The microcarriers were washed, dried for 48 h at 70°C, and weighed. Alternatively, the cells could be detached from the carriers by trypsinization as described in the Results section.

The glucose concentration in the medium was determined enzymatically, using a commercial automatic analyzer (Ebio Compact; Eppendorf, Hamburg, Germany) according to the manufacturer's instructions.

For cell cycle analysis, cells either from tissue flasks or from microcarriers were trypsinized, centrifuged (10 min at 200g), resuspended, fixed in 70% ethanol, and stored at -20°C until measurement. Before measurement the cells were centrifuged and resuspended in PBS. After staining and incubation with propidium iodide (18  $\mu\text{g}/\text{mL}/10^6$  cells) and ribonuclease (40  $\mu\text{g}/\text{mL}/10^6$  cells) for 1 h, analysis was performed with an Epics XL flow cytometer (excitation at 488 nm, emission at 630 nm; Coulter, Krefeld, Germany). DNA histograms were analyzed by a computer model (MultiCycle; Phoenix Flow Systems, San Diego, CA). The S-phase compartment of the cell cultures was used as a parameter for the proliferative activity of the cells.

For each determination of the cell-specific radiotracer uptake, 3 carrier samples (0.25 mL) were taken from the fluidized bed. Each sample was washed 3 times with PBS. The radioactivity (cpm; decay-corrected with half-life  $[t_{1/2}] = 109.7$  min) was measured

using a Gammazint BF 5300 (Berthold, Bad Wildbad, Germany). The sample was subsequently dried and weighed.

#### Determination of LC

The LC, the conversion factor between the utilization of FDG and glucose in cells, was determined as the ratio of the metabolic rates of FDG and glucose (Eq. 1). FDG utilization was calculated from the intracellular uptake measured in the carrier samples during the first 15 min of the experiment:

$$MR_{\text{FDG}} = \frac{q}{A_{\text{sp}}} \left[ \frac{\text{mmol}}{\text{min} \times 10^6 \text{ cells}} \right], \quad \text{Eq. 2}$$

where  $q$  = cell-specific radiotracer uptake rate (cpm/ $10^6$  cells), and  $A_{\text{sp}}$  = specific activity (cpm/mmol glucose). The cell-specific glucose utilization was determined at the same time from analyzed medium samples under steady-state conditions:

$$MR_{\text{Glc}} = \frac{\text{MFR} \times (C_0 - C_r)}{N_t} \left[ \frac{\text{mmol}}{\text{min} \times 10^6 \text{ cells}} \right], \quad \text{Eq. 3}$$

where MFR = medium feed rate (mL/min),  $C_0$  = glucose concentration fresh medium (mmol/L),  $C_r$  = glucose concentration reactor (mmol/L), and  $N_t$  = total number of cells in the reactor.

FDG was synthesized as described (27). The average specific activity was  $<7.4 \times 10^{13}$  Bq/mmol.

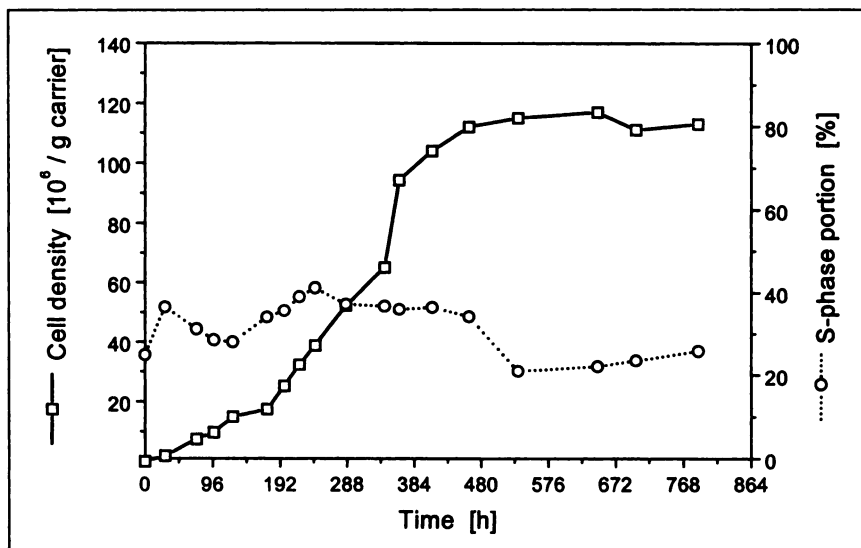


**FIGURE 2.** Cell density during continuous cultivation of 86HG39 glioma cells in fluidized-bed bioreactor.  $\square$  = Number of immobilized cells/g carrier;  $\circ$  = S-phase portion as parameter for proliferative activity of culture.

## RESULTS

### Cultivation in Tissue Flask and Fluidized-Bed Bioreactor

Figure 2 shows the results of a continuous cultivation of 86HG39 glioma cells in the fluidized-bed reactor. The bioreactor was inoculated with  $3 \times 10^6$  viable cells/mL. Within 30 min all cells were immobilized on the carriers in the fluidized bed (data not shown). Carrier samples were used to determine cell density (cells/g carrier) and S-phase portion as parameters for the proliferative activity of the immobilized cells as described above.

After a short lag phase, the number of immobilized cells increased exponentially until the carriers were completely covered with cells. The number of immobilized cells reached a steady-state value of  $1.15 \times 10^8$  cells/g carrier (1 g carrier is approximately equivalent to 2 mL settled carriers). The cells formed a 3-dimensional tumor-like culture (Fig. 3) but were still proliferating, as shown by the S-phase portion, which varied from 40% during the exponential phase to 25% in the steady state. Because of limited space on the carriers, the newly built cells left the carriers and were continuously washed out with the supernatant. This steady state could be maintained for up to 2 mo (data not shown). The MFR remained constant, as did the composition of the supernatant. An S-phase portion of 25%–40% was equivalent to the corresponding value during the exponential growth phase of a batch cultivation of 86HG39 glioma cells in tissue flasks, as shown in Figure 4.

### Cell Detachment from Carriers

An important requirement for examination of the immobilized cells and for determination of cell-specific parameters is a technique that enables complete detachment of the immobilized cells without cellular destruction. This can be performed enzymatically using trypsin. Approximately 0.5 mL carriers with immobilized cells were washed once with PBS and incubated with 2 mL trypsin solution (2.5 g/L; Gibco/BRL) at 37°C. The detached cells were quantified using the erythrosin B exclusion method (26). The total

number of immobilized cells was determined using the crystal violet method. Figure 5 shows the portion of detached cells and their viability in dependence on the time of incubation. After 10 min, all cells were detached within the scope of the accuracy of measurement. A longer incubation resulted in a slight decrease in the number of counted cells, caused by enzymatic lysis of cells. The viability was nearly constant at 85%.

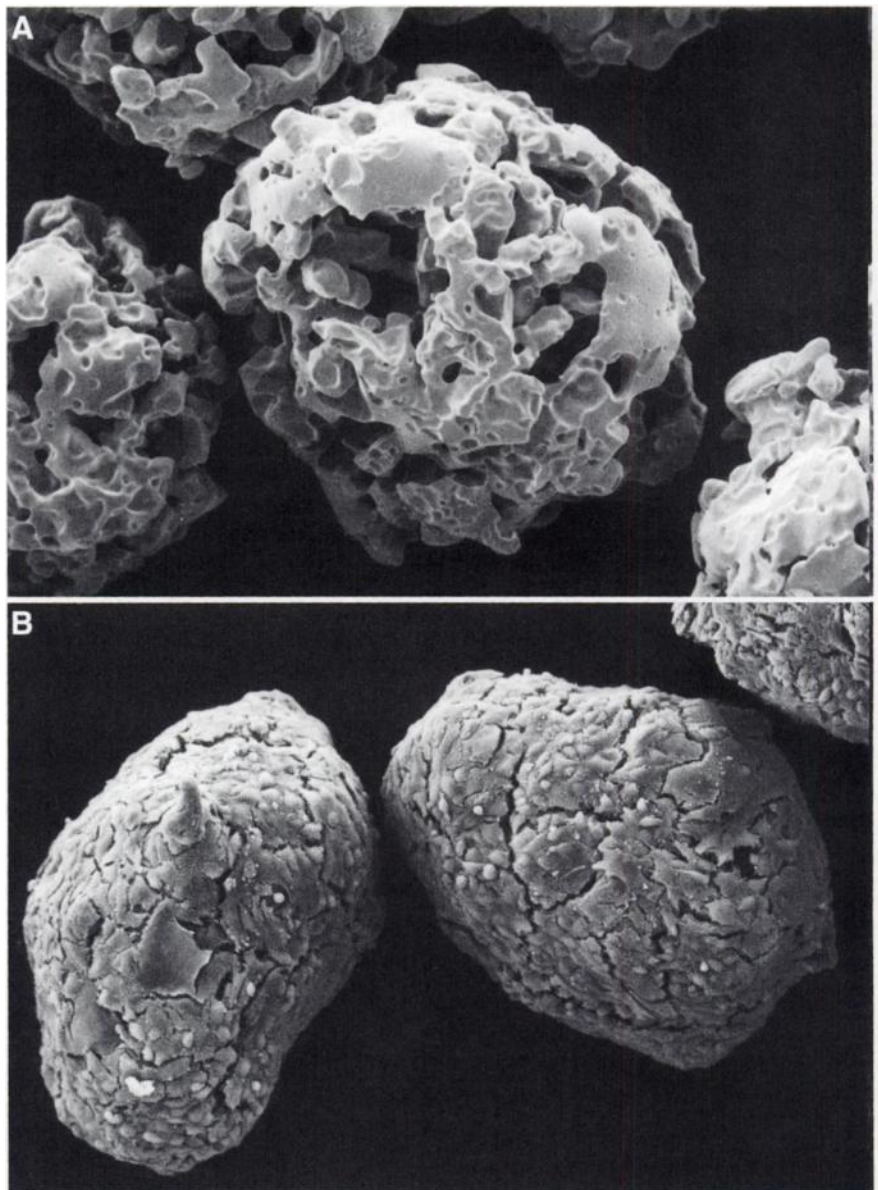
### FDG Uptake of Immobilized Glioma Cells in Fluidized-Bed Bioreactor

Figure 6 shows a transport experiment using FDG in the fluidized-bed bioreactor and performed at the steady state of the fermentation. The glucose concentration in the medium was 3.2 mmol/L, and the MFR was 13 mL/h. At the marked time, a step change in FDG concentration was performed with a final concentration of 0.1 MBq/mL. Fresh medium was also supplemented with 0.1 MBq/mL FDG to avoid dilution effects. Figure 6A shows the on-line signals of the 2 detectors. The lower activity in the fluidized bed is caused by the glass portion of the carriers, which replace activity-containing medium. But because borosilicate glass carriers do not enrich FDG (e.g., by adhesion phenomena), this is a constant effect. Therefore, it can be mathematically corrected using the activity values of the 2 detectors measured immediately after finishing the step input. At this time, the intracellular uptake is negligible, and the quotient of the 2 signals represents the glass portion in the fluidized bed:

$$\text{glass portion} = 100 - \frac{A_{fb}}{A_m} [\%], \quad \text{Eq. 4}$$

where  $A_{fb}$  = radioactivity in the fluidized bed (Bq), and  $A_m$  = radioactivity in the medium (Bq).

Figure 6B shows the on-line signals after decay correction ( $t_{1/2}$  of  $^{18}\text{F}$  = 109.7 min) and mathematical consideration of the glass portion in the fluidized bed. The FDG concentration in the circulating medium was nearly constant, whereas the value in the fluidized bed increased as a result of the



**FIGURE 3.** Scattered-electron microscopy pictures from open porous glass carriers, diameter 400–500  $\mu\text{m}$ , modified with gelatin. (A) Cell-free carrier. (B) Carrier with immobilized cells ( $1.15 \times 10^8$  cells/g carrier).

intracellular enrichment. At different times, carrier and medium samples were taken from the reactor and analyzed for determination of intracellular tracer accumulation, glucose consumption rate, and tracer concentration in the medium. A good correlation between on-line difference signal (difference between both detector signals in Figure 6B) and off-line analyzed samples was obtained (Fig. 6C). The glucose consumption rate was determined to be  $200 \pm 5.5$  ng/ $10^6$  cells/min, and the LC was  $1.14 \pm 0.05$ .

To investigate the dependence of the LC on the glucose concentration in vitro for FDG, 7 experiments with different steady-state levels corresponding to different glucose concentrations in the medium (2.7–12.33 mmol/L) were performed. Figure 7 shows the results for the LC compared with the values obtained from Sokoloff et al. (20) and Suda et al. (23) for [ $^{14}\text{C}$ ]-2-deoxyglucose in rats. For glucose concentrations above 5 mmol/L the LC was found to be in the range of 0.7

$\pm 0.1$ , whereas with glucose concentrations below 5 mmol/L, the LC increased progressively up to a value of  $1.22 \pm 0.01$  at a glucose concentration of 2.7 mmol/L.

## DISCUSSION

The specific goal of this study was to develop and validate a fluidized-bed cell-culture reactor as an in vitro model for the on-line evaluation of radiopharmaceuticals. A human glioma cell line was chosen as the cellular model for this approach. The cells, immobilized in open porous microcarriers, formed stable 3-dimensional spheroids and were continuously proliferating, comparable to cells in the exponential growth phase during batch cultivation.

For examination of the immobilized cells and determination of cell-specific parameters, a trypsinization method that enabled a complete detachment of the immobilized cells without cellular destruction was introduced.

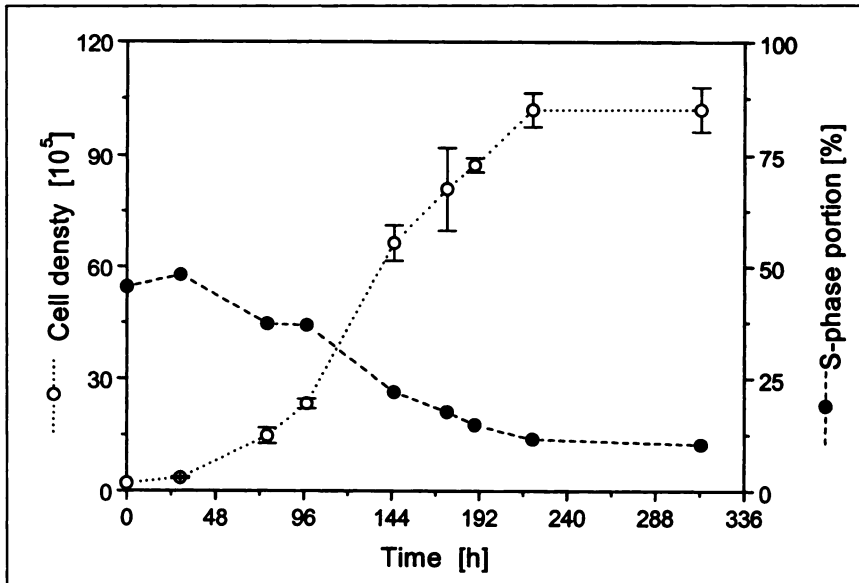


**FIGURE 4.** Batch cultivation of 86HG39 glioma cells in tissue flasks (25 cm<sup>2</sup>). ○ = Number of viable cells; ● = S-phase portion; n = 5.

The fluidized-bed reactor enables consideration of a wide range of experimental setups and offers the advantages of steady-state conditions in a continuous cultivation and with on-line measurement. The long duration of the stable steady state permits a large number of experiments using the same culture over a long time period, provided that the cells are not affected by the experiments. This can be assumed especially for radiotracers. The DO concentration, pH, and medium composition, in addition to temperature, can be adjusted according to the experimental requirements—for example, to examine the effects of heat treatment on cellular transport and metabolism. The flow rate of the circulating medium can be adapted to the flow rate of the blood in the corresponding organism, (e.g., mouse, rat, or human). The input function of the radiotracer is freely adjustable and enables the simulation of in vivo conditions. In contrast to other 3-dimensional systems, such as hollow-fiber or fixed-

bed bioreactors, sampling and examination of the immobilized cells and their compounds are possible at any time. Because of the high cell densities in the bioreactor (total number of cells,  $\sim 1.5 \times 10^9$  viable cells), an easier and more accurate determination of metabolic rates is possible, in comparison with in vitro systems using low cell densities in monolayer cultivation, such as microtiter plates, tissue flasks, or Leighton tubes.

The fluidized-bed bioreactor is suitable for cultivation of a wide spectrum of cells. We performed fermentations with cell lines including hybridoma, Chinese hamster ovary (CHO), baby hamster kidney (BHK), murine mast cells, and different human gliomas, in addition to primary material such as hepatocytes from liver or stromal and hematopoietic cells from bone marrow (12,28,29).

To prove the applicability of this in vitro system, FDG uptake in human glioma cells was examined. The noise of

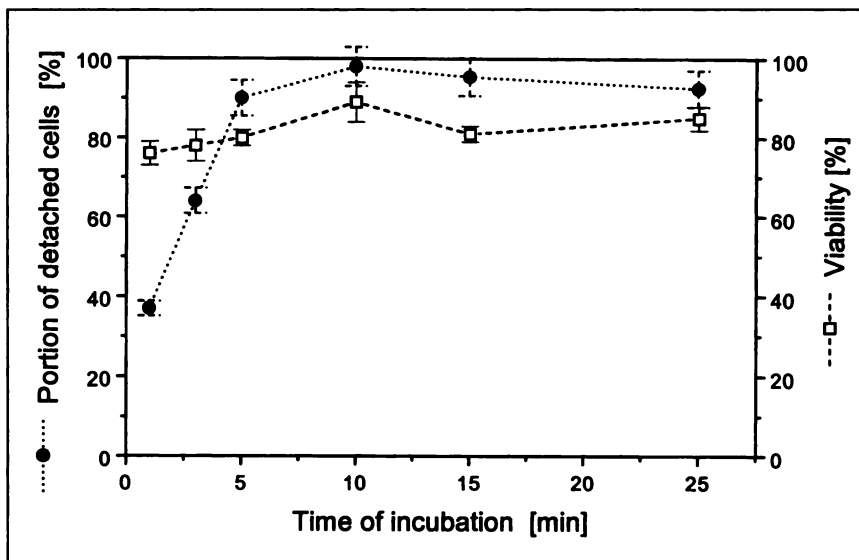


**FIGURE 5.** Enzymatic detachment of 86HG39 glioma cells from carriers with trypsin (2.5 g/L). ● = Portion of detached cells; □ = viability; n = 3.

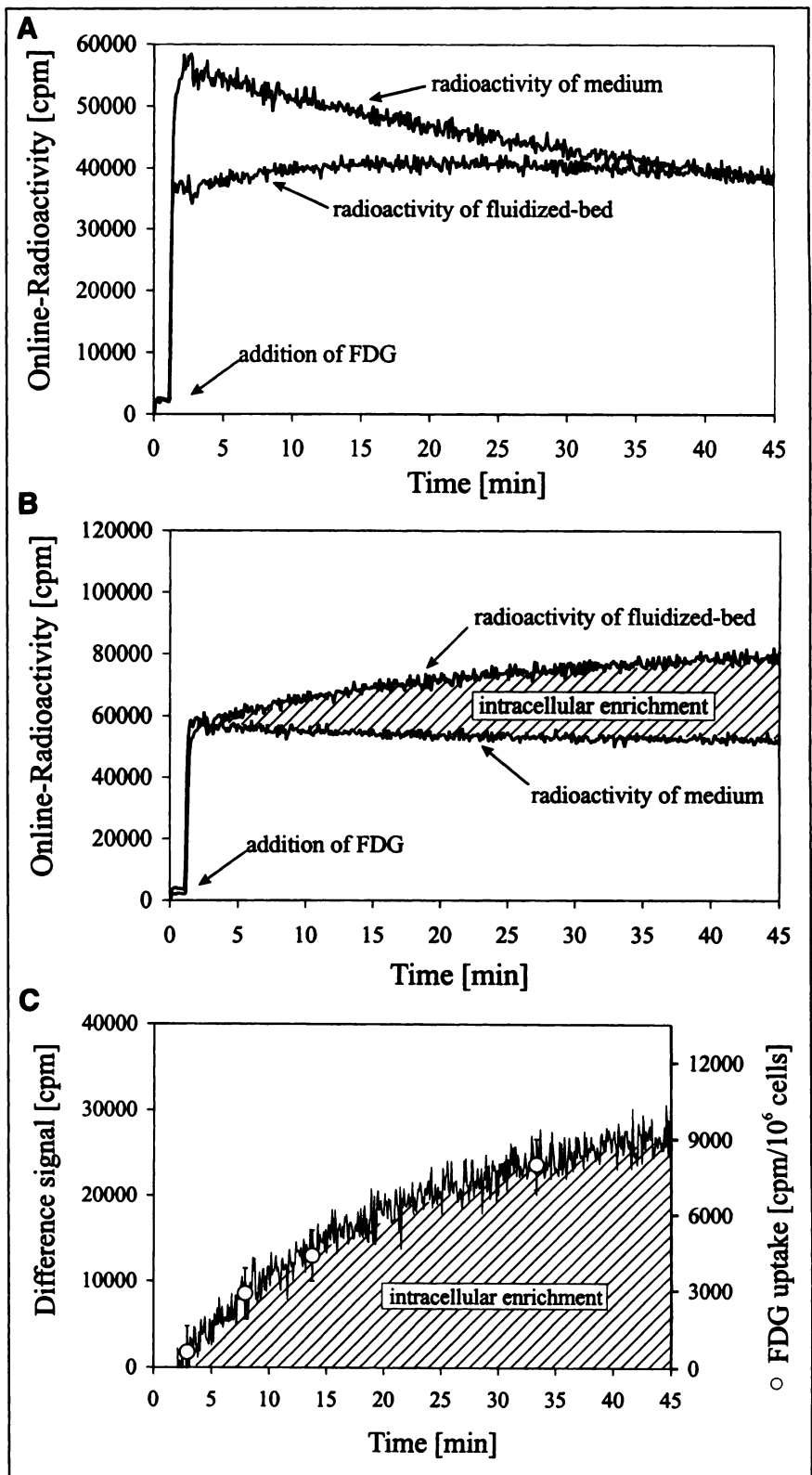


**FIGURE 6.** FDG uptake of  $^{86}\text{HG}39$  glioma cells in fluidized-bed bioreactor. Before starting experiment, cells were cultivated until steady state of number of immobilized cells was reached at  $1.15 \times 10^8$  cells/g carrier. (A) Time course of radioactivity signals measured in medium and fluidized bed after step input of FDG yielding radioactivity concentration of 0.1 MBq/mL. (B) Decay-corrected time-activity signals measured in medium and fluidized bed, allowing calculation of intracellular FDG accumulation. (C) Comparison of intracellular FDG accumulation, obtained by on-line radioactivity detection, with off-line analyzed samples ( $n = 3$ ).

the on-line signal is caused by the fluidization of the carriers. Detector 2 measures a limited volume of the fluidized bed with fluctuation of local carrier density (Fig. 1). The number of cells in this volume depends on the size and porosity of the carriers and on the cell density per g carrier as well as on

the expansion of the fluidized bed (dependent on the flow rate of the circulating medium). Therefore, detector 2 cannot measure the cell-specific uptake directly, and 1 carrier sample per experiment is necessary for calibration. This sample can also be used for further analysis. After calibra-

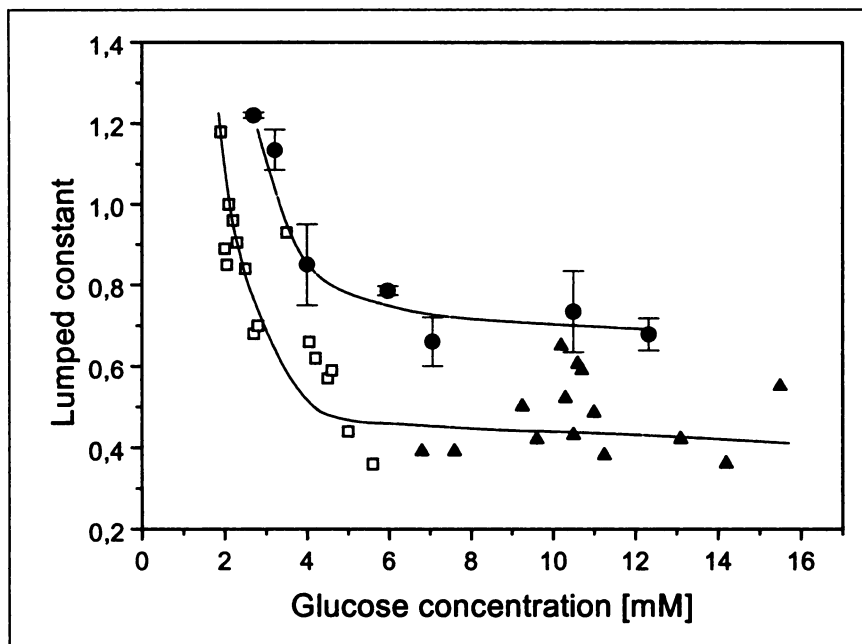


**FIGURE 7.** Values of LC  $\pm$  SD ( $n = 3$ ) at different glucose concentrations: those determined in this study ( $\bullet$ ), normoglycemia in rats using [ $^{14}$ C]-2-deoxyglucose ( $\blacktriangle$ ) (Sokoloff et al. (20)), and hypoglycemia using [ $^{14}$ C]-2-deoxyglucose ( $\square$ ) (Suda et al. (23)). Because there was no obvious mathematical function to fit the observed relationship between LC and glucose concentration, continuous lines were drawn by inspection by Suda et al. (23) and by ourselves, respectively.

tion it was shown by off-line analyzed carrier samples that the intracellular radiotracer uptake is measurable on-line with this system.

To test the potential of the fluidized-bed cell-culture reactor we have analyzed the influence of the glucose concentration on the LC of FDG. Sokoloff et al. (20) and Suda et al. (23) described the influence of the plasma glucose level on the LC of [ $^{14}$ C]-2-deoxyglucose in vivo in rat brain. LC values were described in the literature to be higher in hypoglycemia and to decline from a value of 1.2 for the lowest arterial plasma glucose concentration (1.9 mmol/L) to a constant value of about 0.48 in normoglycemia. Thus, our evidence suggests that the LC of FDG is dependent on the plasma glucose concentration in human glioma cells. For glucose concentrations above 5 mmol/L, the LC was found to be in the range of 0.7, whereas with glucose concentrations below 5 mmol/L, the LC increased up to a value of 1.2 at a glucose concentration of 3 mmol/L. The significantly higher value for the LC in normoglycemia in gliomas compared with normal brain has also been described in other studies of rat (30,31) and human gliomas (21). Earlier studies assumed the LC for gliomas to be the same as that for normal brain (16,32), estimated to be 0.42 (18) or 0.52 (19). But the LC also varies widely from tumor to tumor, as shown by Spence et al. (17), who performed a study including 40 patients with supratentorial malignant gliomas and found the LC to be in a range of 0.72–3.1.

#### Limitations of the Bioreactor

The fluidized-bed bioreactor described is a simplified in vivo model for an organ or a tumor that has no blood vessels or a blood-brain barrier. Furthermore, this system cannot provide information regarding interaction of different cell types or the influence of metabolism of radiopharmaceuticals by other organs, such as the liver. Nevertheless, this

method may improve and enlarge the possibilities of in vitro methods and therefore contribute to a further reduction of the number of animals used for pharmacologic and toxicologic testing.

#### CONCLUSION

The fluidized-bed cell-culture reactor for on-line evaluation of radiotracers in vitro combines precise and flexible control of experimental conditions and physiologic, 3-dimensional cell cultivation with an on-line radioactivity detection system. Using this system we studied the kinetics of FDG in human glioma cells and showed that the dependence of the LC of FDG on the glucose level is similar to that obtained in rat brain studies.

#### ACKNOWLEDGMENTS

The authors thank Prof. Dr. Christian Wandrey for his excellent support of this work and Marcus Cremer for technical assistance.

#### REFERENCES

1. Goldberg AM, Frazier JM. Alternatives to animals in toxicity testing. *Sci Am.* 1989;261:24–30.
2. Shuler ML, Ghanem A, Quick D, Wong MC, Miller P. A self-regulating cell culture analog device to mimic animal and human toxicological responses. *Biotechnol Bioeng.* 1996;52:45–60.
3. Del Raso NJ. In vitro methodologies for enhanced toxicity testing. *Toxicol Lett.* 1993;68:91–99.
4. Frazier JM. In vitro models for toxicological research and testing. *Toxicol Lett.* 1993;68:73–90.
5. Edgington SM. 3-D biotech: tissue engineering. *Bio/Technology.* 1992;10:855–860.
6. Glimelius B, Norling B, Nederman T, Carlsson J. Extracellular matrices in multicellular spheroids of human glioma origin: increased incorporation of proteoglycans and fibronectin as compared to monolayer cultures. *APMIS.* 1988;96:433–444.

7. Gospodarowicz D, Greenburg G, Birdwell CR. Determination of cellular shape by the extracellular matrix and its correlation with the control of cellular growth. *Cancer Res.* 1978;38:4155-4171.
8. Loring J, Glimelius B, Weston JA. Extracellular matrix materials influence quail neural crest cell differentiation in vitro. *Dev Biol.* 1982;90:165-174.
9. West GW, Weichselbaum R, Little JB. Limited penetration of methotrexate into human osteosarcoma spheroids as a proposed model for solid tumor resistance to adjuvant chemotherapy. *Cancer Res.* 1980;40:3665-3668.
10. Nederman T, Norling B, Glimelius B, Carlsson J, Brunk U. Demonstration of an extracellular matrix in multicellular tumor spheroids. *Cancer Res.* 1984;44:3090-3097.
11. Born C, Biselli M, Wandrey C. Production of monoclonal antibodies in a pilot scale fluidized bed bioreactor. In: Beuvery EC, Griffiths JB, Zeijlemaker WP, eds. *Animal Cell Technology: Developments Towards the 21<sup>st</sup> Century*. Boston, MA: Kluwer Academic Publishing; 1995:683-686.
12. Zeng S, Dinter A, Eisenkrätzer D, Biselli M, Wandrey C, Berger EG. Pilot scale expression and purification of soluble protein A tagged  $\beta$ 1,6N-acetyl-glucosaminyltransferase in CHO cells. *Biochem Biophys Res Commun.* 1997;237:653-658.
13. Saha GB, MacIntyre WJ, Go RT. Radiopharmaceuticals for brain imaging. *Semin Nucl Med.* 1994;24:324-349.
14. Alavi JB, Alavi A, Chawluk J, et al. Positron emission tomography in patients with glioma: a predictor of prognosis. *Cancer.* 1988;62:1074-1078.
15. Coleman RE, Hoffman JM, Hanson MW, Sostman HD, Schold SC. Clinical application of PET for the evaluation of brain tumors. *J Nucl Med.* 1991;32:616-622.
16. Di Chiro G. Positron emission tomography using [<sup>18</sup>F]fluorodeoxyglucose in brain tumors: a powerful diagnostic and prognostic tool. *Invest Radiol.* 1987;22:360-371.
17. Spence AM, Muzi M, Graham MM, et al. Glucose metabolism in human malignant gliomas measured quantitatively with PET, 1-[C-11]glucose and FDG: analysis of the FDG lumped constant. *J Nucl Med.* 1998;39:440-448.
18. Phelps ME, Huang SC, Hoffman EJ, Selin C, Sokoloff L, Kuhl DE. Tomographic measurement of local cerebral glucose metabolic rate in humans with (F-18)2-fluoro-2-deoxy-D-glucose: validation of method. *Ann Neurol.* 1979;6:371-388.
19. Reivich M, Alavi A, Wolf A, et al. Glucose metabolic rate kinetic model parameter determination in humans: the lumped constants and rate constants for [<sup>18</sup>F]fluorodeoxyglucose and [<sup>11</sup>C]deoxyglucose. *J Cereb Blood Flow Metab.* 1985;5:179-192.
20. Sokoloff L, Reivich M, Kennedy C, et al. The [<sup>14</sup>C]deoxyglucose method for the measurement of local cerebral glucose utilization: theory, procedure and normal values in the conscious and anesthetized albino rat. *J Neurochem.* 1977;28:897-916.
21. Lear JL, Ackermann RF. Regional comparison of the lumped constants of deoxyglucose and fluorodeoxyglucose. *Metab Brain Dis.* 1989;4:95-104.
22. Mori K, Cruz N, Diemel G, Nelson T, Sokoloff L. Direct chemical measurement of the  $\lambda$  of the lumped constant of the [<sup>14</sup>C]deoxyglucose method in rat brain: effects of arterial plasma glucose level on the distribution spaces of [<sup>14</sup>C]deoxyglucose and glucose and on  $\lambda$ . *J Cereb Blood Flow Metab.* 1989;9:304-314.
23. Suda S, Shinohara M, Miyaoka M, Lucignani G, Kennedy C, Sokoloff L. The lumped constant of the deoxyglucose method in hypoglycemia: effects of moderate hypoglycemia on local cerebral glucose utilization in the rat. *J Cereb Blood Flow Metab.* 1990;10:499-509.
24. Bilzer T, Stavrou D, Dahme E, et al. Morphological, immunocytochemical and growth characteristics of three human glioblastomas established in vitro. *Virchows Arch A Pathol Anat.* 1990;418:281-293.
25. Lüllau E, Dreisbach C, Grogg A, Biselli M, Wandrey C. In: Spier RE, Griffiths JB, MacDonald C, eds. *Animal Cell Technology*. Oxford, UK: Butterworth-Heinemann; 1992:469-475.
26. Phillips HJ. Dye exclusion tests for cell viability. In: Kruse PF, Patterson MK, eds. *Tissue Culture*. New York, NY: Academic Press; 1973:406-408.
27. Hamacher K, Blessing G, Nebeling B. Computer-aided synthesis (CAS) of no-carrier added 2-[<sup>18</sup>F]fluoro-2-deoxyglucose: an efficient automated system for the amino polyether-supported nucleophilic fluorination. *J Appl Radiat Isot.* 1990;41:49-65.
28. Thömmes J, Gätgens J, Biselli M, Runstadler PW, Wandrey C. The influence of dissolved oxygen tension on the metabolic activity of an immobilized hybridoma population. *Cytotechnology.* 1994;13:29-39.
29. Schröder B, Herfurth C, Biselli M, et al. Cocultivation of hematopoietic cells in a fluidized bed reactor. In: Funatsu K, Shirai Y, Matsushita T, eds. *Animal Cell Technology: Basic and Applied Aspects*. Boston, MA: Kluwer Academic Publishing; 1996:137-141.
30. Kapoor R, Spence AM, Muzi M, Graham MM, Abbott GL, Krohn KA. Determination of the deoxyglucose and glucose phosphorylation ratio and the lumped constant in rat brain and transplantable rat glioma. *J Neurochem.* 1989;53:37-44.
31. Spence AM, Graham MM, Muzi M, et al. Deoxyglucose lumped constant estimated in a transplanted rat astrocytic glioma by the hexose utilization index. *J Cereb Blood Flow Metab.* 1990;10:190-198.
32. Tyler JL, Diksic M, Villemure J-G, et al. Metabolic and hemodynamic evaluation of gliomas using positron emission tomography. *J Nucl Med.* 1987;28:1123-1133.